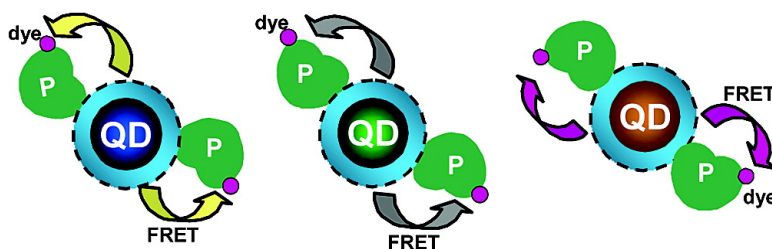![JACS - JOURNAL OF THE AMERICAN CHEMICAL SOCIETY]

Article

Quantum Dot-Based Multiplexed Fluorescence Resonance Energy Transfer

Aaron R. Clapp, Igor L. Medintz, H. Tetsuo Uyeda, Brent R. Fisher, Ellen R. Goldman, Moungi G. Bawendi, and Hedi Mattoussi

More About This Article

Additional resources and features associated with this article are available within the HTML version:

- Supporting Information
- Links to the 24 articles that cite this article, as of the time of this article download
- Access to high resolution figures
- Links to articles and content related to this article
- Copyright permission to reproduce figures and/or text from this article

View the Full Text HTML

Quantum Dot-Based Multiplexed Fluorescence Resonance Energy Transfer

Aaron R. Clapp,[†] Igor L. Medintz,[‡] H. Tetsuo Uyeda,[†] Brent R. Fisher,[§]
Ellen R. Goldman,[‡] Moungi G. Bawendi,[§] and Hedi Mattoussi[†,*]

*Contribution from the U.S. Naval Research Laboratory, Optical Sciences Division, Code 5611,
Washington, D.C. 20375, U.S. Naval Research Laboratory, Center for Bio/Molecular Science
and Engineering, Code 6900, Washington, D.C. 20375, and Department of Chemistry,
Massachusetts Institute of Technology, Cambridge, Massachusetts 02139*

Received August 4, 2005; E-mail: hedimat@ccs.nrl.navy.mil

Abstract: We demonstrate the use of luminescent quantum dots (QDs) conjugated to dye-labeled protein acceptors for nonradiative energy transfer in a multiplexed format. Two configurations were explored: (1) a single color QD interacting with multiple distinct acceptors and (2) multiple donor populations interacting with one type of acceptor. In both cases, we showed that simultaneous energy transfer between donors and proximal acceptors can be measured. However, data analysis was simpler for the configuration where multiple QD donors are used in conjunction with one acceptor. Steady-state fluorescence results were corroborated by time-resolved measurements where selective shortening of QD lifetime was measured only for populations that were selectively engaged in nonradiative energy transfer.

Introduction

The development of rapid and sensitive assays for the accurate detection of toxins and small molecule analytes in soil, water, and food supplies is a continuing goal with numerous applications in food and health care industries, including screenings and diagnostics. To improve the speed and efficiency of fluorescence-based detection assays, there has been a strong motivation to devise parallel detection methods based on the simultaneous measurement of two or more specific fluorescence signals. Previously, these methods used organic dyes to generate independent signal channels, each corresponding to a particular target molecule. Several examples of multiplexed dye-based assays exist in the literature, including a fluorescence-linked immunosorbent assay (FLISA)[3] and numerous advanced flow cytometry-based techniques.[4−9] However, due to the narrow absorption and red-tailed emission spectra of organic dyes and fluorescent proteins, simultaneous detection of multiple signals is complicated, often requiring several excitation sources and a complex arrangement of filters to produce independent signal channels with reduced cross-talk.[10] Additionally, due to the susceptibility of organic dyes to photodegradation, extended illumination can significantly reduce the fluorescence signal, which limits their use in designing assays for continuous sample monitoring.

Luminescent semiconductor quantum dots (QDs) have shown great promise as potential replacements for traditional organic fluorophores in several biotechnological applications.[11−22] Some of the inherent advantages over organic dyes include a strong resistance to chemical and photodegradation, large absorption cross sections over a broad range of excitation wavelengths, and tunable emission profiles. In particular, CdSe−ZnS core−

[†] U.S. Naval Research Laboratory, Optical Sciences Division.
[‡] U.S. Naval Research Laboratory, Center for Bio/Molecular Science and Engineering.
[§] Massachusetts Institute of Technology.
(1) Wolfbeis, O. S. *Anal. Chem.* **2004**, *76*, 3269−3283.
(2) Monk, D. J.; Walt, D. R. *Anal. Bioanal. Chem.* **2004**, *379*, 931−945.
(3) Swartzman, E. E.; Miraglia, S. J.; Mellentin-Michelotti, J.; Evangelista, L.; Yuan, P. M. *Anal. Biochem.* **1999**, *271*, 143−151.
(4) Roederer, M.; DeRosa, S.; Gerstein, R.; Anderson, M.; Bigos, M.; Stovel, R.; Nozaki, T.; Parks, D.; Herzenberg, L.; Herzenberg, L. *Cytometry* **1997**, *29*, 328−339.
(5) Szollosi, J.; Damjanovich, S.; Matyus, L. *Cytometry* **1998**, *34*, 159−179.
(6) Fulton, R. J.; McDade, R. L.; Smith, P. L.; Kienker, L. J.; Kettman, J. R. *Clin. Chem.* **1997**, *43*, 1749−1756.
(7) Kellar, K. L.; Iannone, M. A. *Exp. Hematol.* **2002**, *30*, 1227−1237.
(8) Chan, F. K. *Methods Mol. Biol.* **2004**, *261*, 371−82.
(9) Becker, S.; Schmoldt, H. U.; Adams, T. M.; Wilhelm, S.; Kolmar, H. *Curr. Opin. Biotechnol.* **2004**, *15*, 323−329.
(10) Schröck, E.; du Manoir, S.; Veldman, T.; Schoell, B.; Wienberg, J.; Ferguson-Smith, M. A.; Ning, Y.; Ledbetter, D. H.; Bar-Am, I.; Soenksen, D.; Garini, Y.; Ried, T. *Science* **1996**, *273*, 494−497.
(11) Bruchez, M.; Moronne, M.; Gin, P.; Weiss, S.; Alivisatos, A. P. *Science* **1998**, *281*, 2013−2016.
(12) Chan, W. C. W.; Nie, S. *Science* **1998**, *281*, 2016−2018.
(13) Mattoussi, H.; Mauro, J. M.; Goldman, E. R.; Anderson, G. P.; Sundar, V. C.; Mikulec, F. V.; Bawendi, M. G. *J. Am. Chem. Soc.* **2000**, *122*, 12142−12150.
(14) Dubertret, B.; Skourides, P.; Norris, D. J.; Noireaux, V.; Brivanlou, A. H.; Libchaber, A. *Science* **2002**, *298*, 1759−1762.
(15) Wu, X.; Liu, H.; Liu, J.; Haley, K. N.; Treadway, J. A.; Larson, J. P.; Ge, N.; Peale, F.; Bruchez, M. P., Jr. *Nat. Biotechnol.* **2003**, *21*, 41−46.
(16) Jaiswal, J. K.; Mattoussi, H.; Mauro, J. M.; Simon, S. M. *Nat. Biotechnol.* **2003**, *21*, 47−51.
(17) Kim, S.; Lim, Y. T.; Soltesz, E. G.; De Grand, A. M.; Lee, J.; Nakayama, A.; Parker, J. A.; Mihaljevic, T.; Laurence, R. G.; Dor, D. M.; Cohn, L. H.; Bawendi, M. G.; Frangioni, J. V. *Nat. Biotechnol.* **2004**, *22*, 93−97.
(18) Medintz, I. L.; Clapp, A. R.; Mattoussi, H.; Goldman, E. R.; Fisher, B. M.; Mauro, J. M. *Nat. Mater.* **2003**, *2*, 630−638.
(19) Goldman, E. R.; Clapp, A. R.; Anderson, G. P.; Uyeda, H. T.; Mauro, J. M.; Medintz, I. L.; Mattoussi, H. *Anal. Chem.* **2004**, *76*, 684−688.
(20) Michalet, X.; Pinaud, F. F.; Bentolila, L. A.; Tsay, J. M.; Doose, S.; Li. J. J.; Sundaresan, G.; Wu, A. M.; Gambhir, S. S.; Weiss, S. *Science* **2005**, *307*, 538−544.
(21) Medintz, I. L.; Uyeda, H. T.; Goldman, E. R.; Mattoussi, H. *Nat. Mater.* **2005**, *4*, 435−446.
(22) Parak, W. J.; Pellegrino, T.; Plank, C. *Nanotechnology* **2005**, *16*, R9−R25.

shell QDs exhibit size-dependent emission spectra with narrow bandwidths over most of the visible spectrum and can be efficiently excited at any wavelength below the absorption band edge (from the visible to well into the UV).[20-22] The ZnS overcoating layer in these core−shell QDs provides improved passivation for the fluorescent core and a stable surface for further chemical processing. As prepared, the QD surface is typically capped with a mixture of hydrophobic ligands that are incompatible with aqueous and biological environments. However, by using properly designed surface functionalities (via either cap exchange or encapsulation), QDs can be readily dispersed in aqueous media thus rendering them biologically compatible for use in a number of applications including site-directed cell labeling, immunoassays and fluorescence resonance energy transfer based assays.[11,15,16,18-22] Despite the limited scope of each of these strategies, substantial overall progress has been made allowing QDs to be dispersed in a variety of aqueous buffers and conjugated with a host of biomolecules (e.g., DNA, proteins), thereby conferring specificity for potential biological targets. Recent reviews describe the current and potential uses of QD fluorophores in a variety of biological applications.[20-22]

Förster (or fluorescence) resonance energy transfer (FRET) applied to luminescent QDs has been investigated extensively by several groups.[18,23-32] In addition to understanding the fundamental aspects of this process applied to these inorganic fluorophores, we have focused on using FRET as a means of characterizing the molecular structure of proteins conjugated to QDs and developing sensing assemblies to detect specific analytes.[18,23-25] We have shown that QDs are excellent energy donors with dye-labeled protein acceptors, where simple tuning of the degree of spectral overlap with a given acceptor can be achieved by adjusting the QD photoemission.[23] Furthermore, because their size is comparable to that of many common proteins, a single QD can efficiently interact with multiple dye-labeled protein acceptors positioned around the QD surface.[23] We have also shown that classical Förster theory accurately describes these interactions and can be used as a quantitative tool to derive information such as donor−acceptor distances.[23] For example, we used QD-based FRET to determine the orientation of surface-bound maltose binding protein (MBP), self-assembled on the nanocrystal surface, and to develop nanoscale biosensors that target either maltose or soluble TNT.[18,24,25]

One of the unique properties of QDs as fluorescence probes is their symmetric and narrow photoemission profile. Unlike conventional dye molecules which have characteristically skewed emission profiles, QDs have Gaussian-like photoluminescence (PL) spectra with typical full widths at half-maximum (fwhm) of about 20 to 35 nm.[33] These symmetric PL profiles are ideal for signal multiplexing, where many fluorescence signals can be measured simultaneously. Additionally, various populations of QDs (each having a unique "color") can be excited with the same monochromatic source (e.g., laser line). We have recently incorporated multiple populations of QDs bound to specific antibodies into surface-bound sandwich fluoroimmunoassays for the simultaneous detection of up to four soluble toxins.[19] In this assay format, each population (color) of QD−antibody conjugates specifically interacts with a target toxin/analyte immobilized on a substrate via a second capture antibody, resulting in a sandwiched structure. This structure does not form in the absence of the specific antibodies or the target toxins. The PL contribution from each subset (color) of QDs indicates sandwich formation and detection of a particular toxin. Deconvolution of the composite PL spectrum (to resolve contributions from individual QD populations) reports the presence of that target analyte and potentially its concentration. A single excitation line was used in these experiments, and no energy transfer was involved.[19] Similarly, a multiplexing technique known as "spectral barcoding" was demonstrated using microspheres impregnated with QDs having different PL spectra and at various loading fractions.[34,35] In this case each microsphere has a specific PL signature, where the overall emission spectrum, along with the relative peak intensities, provide a unique optical code in the mixture. Despite these early examples, the full potential for developing multiplexed assays based on luminescent QDs remains largely unrealized.

In this report, we demonstrate the use of QDs as energy donors in conjunction with dye acceptors to develop multiple FRET interactions that can be quantitatively and simultaneously detected. Several prototype arrangements are examined and evaluated for generating FRET interactions with straightforward data analysis. We examined the case where a single QD donor interacts with multiple dye acceptors and compared it to the "reverse" configuration where multiple QDs donors are used in conjunction with one type of dye acceptor. The advantages and disadvantages of each arrangement are discussed. We also discuss how these results could potentially be applied to develop sensing assemblies capable of providing simultaneous detection of multiple target molecules in solution.

Materials and Methods

Quantum Dot Synthesis. Four populations of CdSe−ZnS core−shell QDs (having PL emission maxima at 510, 555, 570, and 590 nm) were prepared using well-established synthetic techniques consisting of growth and annealing of organometallic precursors at high temperature.[36-39] These QDs were rendered water-soluble by replacing

(23) Clapp, A. R.; Medintz, I. L.; Mauro, J. M.; Fisher, B. R.; Bawendi, M. G.; Mattoussi, H. *J. Am. Chem. Soc.* **2004**, *126*, 301−310.
(24) Medintz, I. L.; Konnert, J. H.; Clapp, A. R.; Stanish, I.; Twigg, M. E.; Mattoussi, H.; Mauro, J. M.; Deschamps, J. R. *Proc. Natl. Acad. Sci. U.S.A.* **2004**, *101*, 9612−9617.
(25) Goldman, E. R.; Medintz, I. L.; Whitley, J. L.; Hayhurst, A.; Clapp, A. R.; Uyeda, H. T.; Deschamps, J. R.; Lassman, M. E.; Mattoussi, H. *J. Am. Chem. Soc.* **2005**, *127*, 6744−6751.
(26) Kagan, C. R.; Murray, C. B.; Bawendi, M. G. *Phys. Rev. B* **1996**, *54*, 8633.
(27) Crooker, S. A.; Hollingsworth, J. A.; Tretiak, S.; Klimov, V. I. *Phys. Rev. Lett.* **2002**, *89*, 186802.
(28) Willard, D. M.; Carillo, L. L.; Jung, J.; Van Orden, A. *Nano Lett.* **2001**, *1*, 469−474.
(29) Tran, P. T.; Goldman, E. R.; Anderson, G. P.; Mauro, J. M.; Mattoussi, H. *Phys. Status Solidi B* **2002**, *229*, 427−432.
(30) Patolsky, F.; Gill, R.; Weizmann, Y.; Mokari, T.; Banin, U.; Willner, I. *J. Am. Chem. Soc.* **2003**, *125*, 13918−13919.
(31) Samia, A. C.; Chen, X.; Burda, C. *J. Am. Chem. Soc.* **2003**, *125*, 15736−15737.
(32) Oh, E.; Hong, M. Y.; Lee, D.; Nam, S. H.; Yoon, H. C.; Kim, H. S. *J. Am. Chem. Soc.* **2005**, *127*, 3270−3271.
(33) Gaponenko, S. V. *Optical Properties of Semiconductor Nanocrystals*; Cambridge University Press: Cambridge, 1998.
(34) Xu, H. X.; Sha, M. Y.; Wong, E. Y.; Uphoff, J.; Xu, Y. H.; Treadway, J. A.; Truong, A.; O'Brien, E.; Asquith, S.; Stubbins, M.; Spurr, N. K.; Lai, E. H.; Mahoney, W. *Nucleic Acids Res.* **2003**, *31*, e43.
(35) Jain, K. K. *Expert Rev. Mol. Diagn.* **2003**, *3*, 153−161.
(36) Murray, C. B.; Norris, D. J.; Bawendi, M. G. *J. Am. Chem. Soc.* **1993**, *115*, 8706−8715.
(37) Peng, Z. A.; Peng, X. *J. Am. Chem. Soc.* **2001**, *123*, 183−184.
(38) Hines, M. A.; Guyot-Sionnest, P. *J. Phys. Chem.* **1996**, *100*, 468−471.
(39) Dabbousi, B. O.; Rodriguez-Viejo, J.; Mikulec, F. V.; Heine, J. R.; Mattoussi, H.; Ober, R.; Jensen, K. F.; Bawendi, M. G. *J. Phys. Chem. B* **1997**, *101*, 9463−9475.

the native hydrophobic trioctylphosphine/trioctylphosphine oxide (TOP/TOPO) organic capping ligands with dihydrolipoic acid (DHLA) using methods described in previous reports.[13,18,21] The DHLA-capped QDs have negatively charged surfaces with uniform distribution, due to the deprotonated carboxylic acid end groups, and are stable in basic buffer solutions.

Maltose Binding Protein. As described in several prior studies,[18,23,24,40] *E. coli* maltose binding protein (MBP) was engineered to express a sequence of five histidine residues at the C-terminus. MBP was labeled with an organic dye at a unique cysteine residue located at position 95 of the amino acid sequence. The protein was reduced with dithiothreiothol (Pierce, Rockford, IL) and reacted with monofunctional maleimide-QSY-7 (a quenching dye) or Cy3 (an emitting dye) (Amersham Pharmacia, Piscataway, NJ). This procedure yielded MBP–QSY-7 and MBP–Cy3 with an average labeling ratio of one dye per protein, determined from the absorption data and using the extinction coefficients of the protein at 280 nm, QSY-7 at 560 nm, and Cy3 at 553 nm. Dye-labeled MBP was purified by column chromatography using PD-10 columns (Amersham Pharmacia) to remove excess free dye.[18,23,24]

Self-Assembly of QD–Protein Conjugates. QD–protein bioconjugates were formed by adding appropriate molar ratios of labeled and unlabeled proteins to 100 μL of sodium tetraborate buffer (pH 9.5) containing DHLA-capped QDs and allowing the mixture to incubate for 15 min at room temperature. Self-assembly of the protein on the QD is driven by metal-affinity coordination between the DHLA-capped surface and the C-terminal histidine tail. This scheme exhibited rapid and stable binding of the protein to QDs in solution.[18,23,24] The self-assembly process was repeated for each QD population, after which the individually assembled samples (each prepared in separate Eppendorf tubes) were mixed together and diluted to a final volume of 3 mL. Regardless of the specific dye-to-QD ratio for a particular preparation, the overall MBP-to-QD ratio was fixed at 15:1 (near saturation), which allows one to maintain a constant quantum yield of the solutions.[13,23] In a self-assembly process, variation in the number of proteins per QD conjugate for a given nominal protein-to-QD ratio obeys a Poisson distribution function.[41] For this reason, the exact number of acceptors per nanocrystal (donor) is difficult to estimate. However, the distribution width narrows when larger protein-to-QD ratios are used. Since our QD conjugates always have a rather large number of proteins (near or at saturation, by mixing labeled and unlabeled proteins), the distribution is not expected to dramatically change the overall ensemble efficiency. This was confirmed in the FRET data collected from experiments using increasing ratios of dye-labeled proteins per QD (for a fixed total number of proteins per nanocrystal), where the measured efficiencies closely matched the expected enhancement due to increasing acceptor-to-donor ratios in each conjugate.[23]

Steady-State and Time-Resolved Fluorescence Measurements and Spectral Decovolution. Steady-state fluorescence spectra were measured with a SPEX Fluorolog-3 fluorimeter (Jobin-Yvon, Edison, NJ) using a 3 mL quartz cuvette (1 cm optical path) and 400 nm excitation. Control spectra from solutions containing only MBP-dye (for Cy3) were subtracted from the composite signal to account for direct excitation. Spectral deconvolution of the steady-state data was performed using a custom algorithm in MATLAB which considered the measured composite signal as the linear combination (superposition) of known QD signals: $I_{total}(\lambda) = \sum_i a_i I_i(\lambda)$ where a_i and $I_i(\lambda)$ are fitting proportionality constants (weighting factors) and the known individual QD emission spectra, respectively. Using standard regression analysis, a best-fit curve was found consisting of representative fractional contributions of each QD PL signal.

(40) Clapp, A. R.; Medintz, I. L.; Fisher, B. R.; Anderson, G. P.; Mattoussi, H. *J. Am. Chem. Soc.* **2005**, *127*, 1242−1250.
(41) Grimmett, G. R.; Stirzaker, D. R. *Probability and Random Processes*, 2nd ed.; Oxford University Press: Oxford, 1992.

Experimentally, energy transfer efficiency can be determined from steady-state fluorescence data as[42]

$$E_{QD-dye} = \frac{F_D - F_{DA}}{F_D} \tag{1}$$

where F_D and F_{DA} designate the donor fluorescence alone and in the presence of the acceptor, respectively. FRET efficiency can also be determined from changes in the donor exciton lifetime when it is engaged in nonradiative energy transfer to a proximal acceptor, using time-resolved fluorescence.[42] For a system having one donor interacting with several acceptors symmetrically placed around its center, the overall energy transfer efficiency is

$$E = \frac{\sum_i^n k_{D-A,i}}{\sum_i^n k_{D-A,i} + \tau_D^{-1}} \tag{2}$$

where n is the total number of surface bound acceptors, $k_{D-A,i}$ are individual rates of nonradiative energy transfer (that depend on the specific D−A pair considered), and τ_D^{-1} is the radiative lifetime of the donor in the absence of acceptors.[23] Equation 2 is general for any single donor/multiple acceptor system yet can be complicated in practice if the acceptors are located at random locations with respect to the donor or if there are multiple types of acceptors involved. If we consider the specific case of multiple identical acceptors equidistant from a central donor, the overall efficiency can be written as

$$E = \frac{n k_{D-A}}{n k_{D-A} + \tau_D^{-1}} = \frac{n R_0^6}{n R_0^6 + r^6} \tag{3}$$

where R_0 is the calculated Förster distance and r is the fixed D−A distance. Given an experimental measurement of the FRET efficiency, eq 3 can be used to determine the D−A distance for a particular system.[23,24]

Fluorescence lifetimes were measured as described previously using a custom-built far-field epifluorescence microscope system with an attached spectrometer, a time-gated cooled CCD detector and a 414 nm pulsed diode laser (5 MHz, 90 ps pulse width, PicoQuant GmbH, Berlin, Germany) for excitation.[18,23] Lifetime data were collected using DaVis software (LaVision GmbH, Göettingen, Germany). Time-resolved fluorescence data were deconvoluted by binning relevant regions of the spectrum characteristic of a particular fluorophore emission and fitting the resulting intensity profile to a biexponential decay function.

Results

Configuration 1: Single QD Donor with Multiple Distinct Dye Acceptors. Here we limit our description to the case of one QD donor and two acceptors. Data and conclusions using three or more acceptors with a single QD donor are consistent with the findings discussed below. Figure 1A shows a schematic representation of a configuration with one QD donor interacting with two distinct acceptor dyes: a QSY-7 quencher and a Cy3 emitter. Relevant QD PL and dye absorption spectra are provided in Figure 2 and cover all of the donor−acceptor pairs considered in this study. 555 nm emitting QDs were self-assembled with MBP−Cy3 and MBP−QSY-7 at several discrete acceptor-to-QD ratios while maintaining the total protein coverage at 15 MBP per QD; unlabeled MBP was added as

(42) Lakowicz, J. R. *Principles of Fluorescence Spectroscopy*, 2nd ed.; Kluwer Academic: New York, 1999.
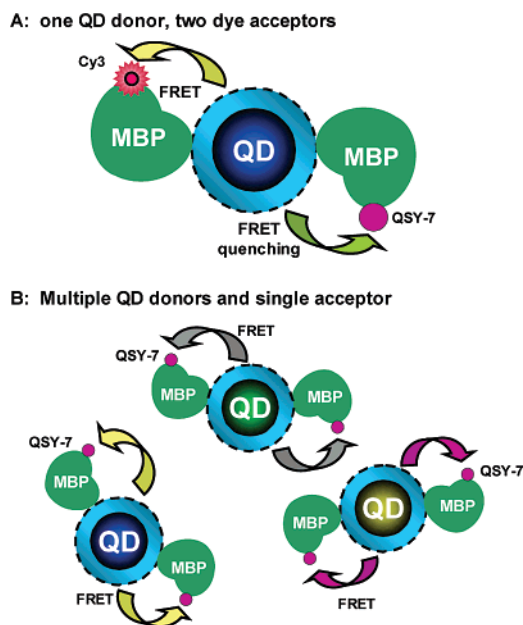
Figure 1. Schematic representation of the FRET multiplexing configurations used in this study. (A) A single QD donor interacting with two different acceptors, MBP—Cy3 (emitting acceptor) and MBP—QSY-7 (dark quencher). (B) Three distinct QD donors conjugated to QSY-7-labeled MBP. For this arrangement, blue, green, and yellow emitting QDs are represented.
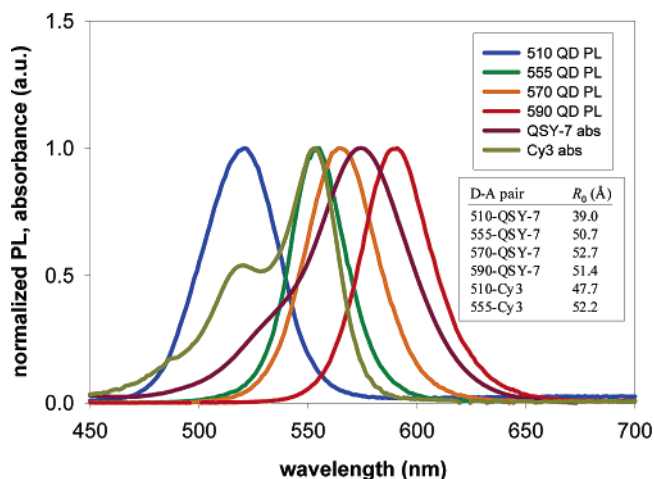

Figure 2. Absorption spectra of the dye acceptors (Cy3 and QSY-7) along with the emission spectra of the various QDs used (emission maxima were at 510, 555, 570, and 590 nm); normalized data are shown. The corresponding Förster distances, R_0, for the various donor—acceptor pairs are also reported in the inserted table.

needed to bring the total protein-to-QD ratio to 15:1. Ratios of QSY-7 and Cy3 per QD explored are: (2 QSY-7, 0 Cy3), (0 QSY-7, 2 Cy3), (2 QSY-7, 2 Cy3), (0 QSY-7, 6 Cy3), (6 QSY-7, 0 Cy3), and (6 QSY-7, 6 Cy3). For clarity, Figure 3A shows the 555 nm QD signal deconvoluted from the Cy3 photoemission (full composite spectra are shown in Supporting Information) for various QSY-7 and Cy3-to-QD ratios. As expected, increasing one or a combination of dye acceptors (thus varying the overall dye-to-QD ratio) decreases the QD PL indicating a systematic increase in FRET efficiency with the total number of acceptors placed around each QD donor. Figure 3B is a color contour plot showing the measured FRET efficiency (E, defined as the fractional donor PL loss in the presence of acceptor) as a function of the ratios of Cy3 and QSY-7 per QD. Note that
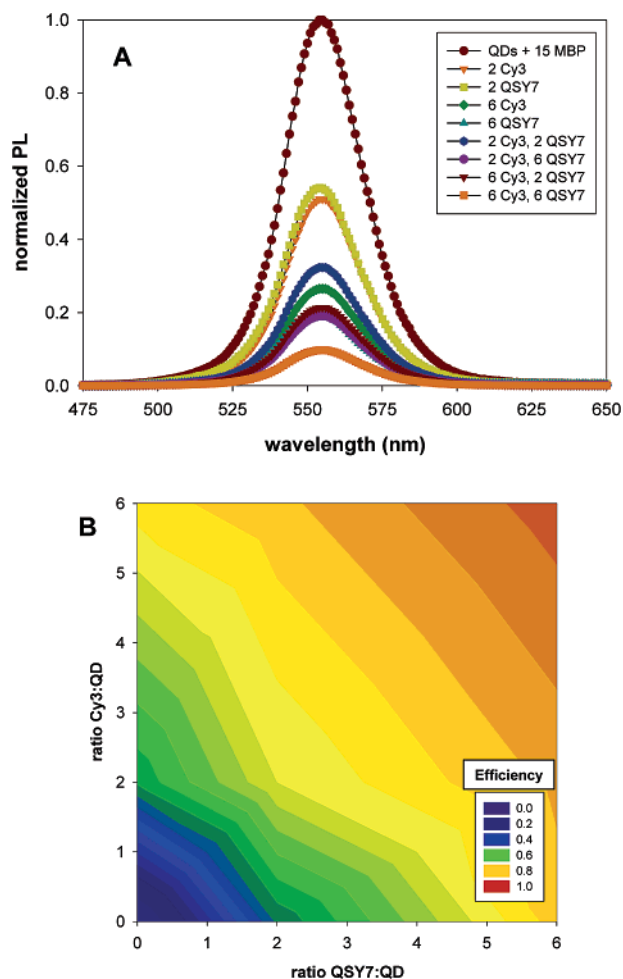

Figure 3. (A) Deconvoluted PL spectra for the single QD donor—two dye acceptor (Cy3 and QSY-7) system at various dye-to-QD ratios; 555 nm emitting QDs are used. The deconvoluted contributions from Cy3 are omitted for clarity. (B) Color-coded contour plot of measured FRET efficiency as a function of Cy3 and QSY-7-to-QD ratios. Data are interpolated to show a continuous variation of efficiency as a function of dye-to-QD ratios.

the measured efficiency is nearly symmetric about the diagonal, indicating a similar transfer efficiency between 555 nm emitting QDs and either Cy3 or QSY-7; this result is consistent with the similar R_0 values reported in Figure 2.

The configuration of a single donor with multiple acceptors, although easily implemented and perhaps obvious from a design standpoint, involves more complex spectral deconvolution and data analysis due to the broad and red-tailed emission from dyes. It requires analysis of both donor and acceptor signals (i.e., QD PL loss and dye PL gain) in order to separate FRET contributions from interactions with different acceptors. Analysis based on donor PL loss alone is insufficient to fully characterize individual nonradiative energy transfer processes in this arrangement. If the acceptors are emissive dyes, the presence of two or more red-tailed PL spectra combined with the possible contribution from inter-dye FRET can greatly complicate data analysis. For these reasons, we investigated an alternative configuration where one type of acceptor dye interacts with multiple populations of QD donors. This configuration is also more practical because several QD emission spectra can fit within the absorption window of an organic dye generating sufficient spectral overlap with all QD donors.
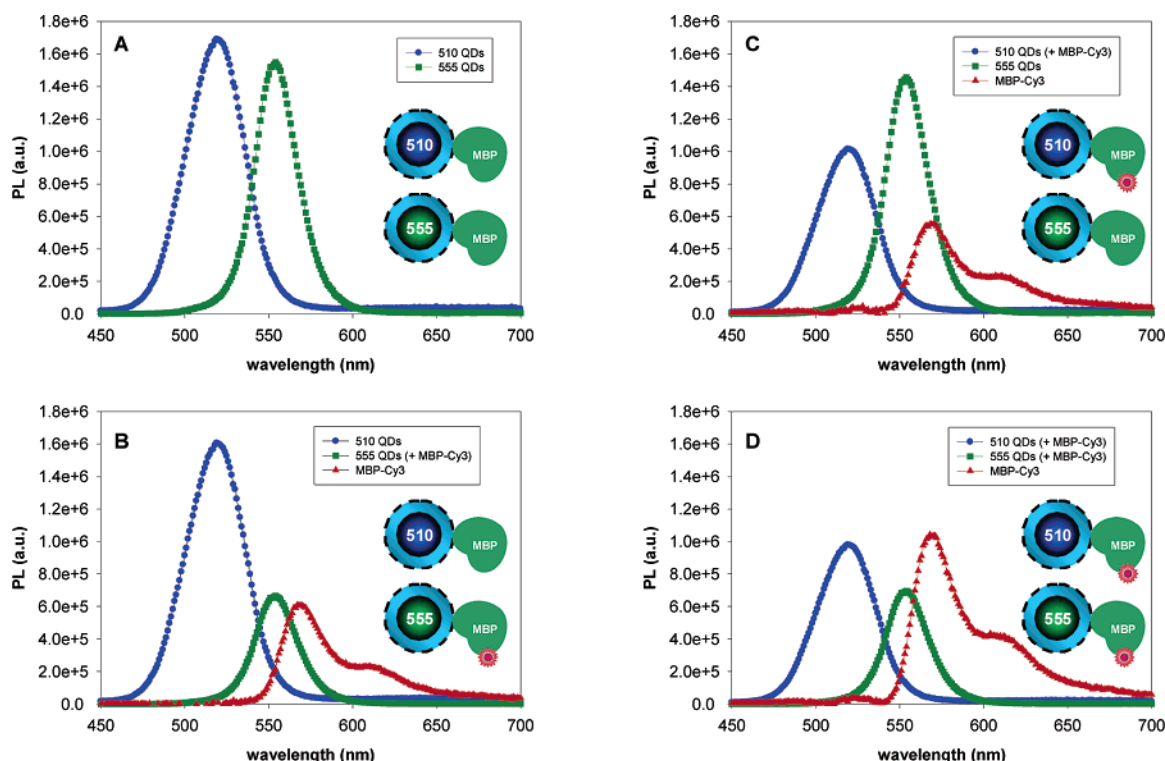
Figure 4. Deconvoluted PL spectra for the system using two QD donors and a Cy3 acceptor. (A) Spectra of 510 and 555 nm QDs, each with 15 unlabeled MBP per QD. (B) Spectra for the 510 nm QDs (with unlabeled MBP) and for 555 nm QDs (with four labeled MBP per QD). (C) Reverse case of (B) where 510 nm QDs have labeled MBP and 555 nm have unlabeled MBP only. (D) Spectra of solutions where both 510 and 555 nm QDs have four MBP−Cy3 per QD. Cartoons representing labeled and unlabeled QD conjugates are shown in the insets.

Configuration 2: Multiple QD Donors with One Acceptor. Figure 1B shows a schematic representation of a configuration where three QD donor populations simultaneously interact with the same acceptor. In this context, we will discuss three separate examples. The first example corresponds to the case of two QD donors interacting with one emitting acceptor (Cy-3). The second and third examples correspond to cases where a single quenching acceptor (QSY-7) interacts with three and four QD donors, respectively.

1. Two QD Donor Populations with Cy3 Dye Acceptor. In this arrangement, 510 and 555 nm emitting QDs were paired with Cy3-labeled MBP as the proximal acceptor, and the entire sample was excited at 400 nm. Figure 4A shows the individual deconvoluted spectra of the QD−MBP solutions (no acceptor present). Figure 4B shows the deconvoluted spectra of the two QDs and Cy3 for a sample where four of the 15 MBP immobilized on the 555 nm emitting QDs are dye-labeled (510 nm QDs are conjugated to unlabeled MBP). While there is a clear decrease in the 555 nm QD signal due to FRET (with an efficiency $E_{555-Cy3} = 0.57$), the 510 nm QD signal is nearly unchanged (∼5% change). A commensurate contribution from the Cy3 acceptor (attributed to FRET) is shown. Figure 4C shows the spectra collected from a sample with the reverse arrangement: 4 of 15 MBP bound to the 510 nm QDs are Cy3-labeled. Here, the 510 nm QD signal shows substantial loss (with a quenching efficiency $E_{510-Cy3} = 0.41$), while the 555 QD signal is nearly unaffected. The dye emission contribution for this pair is smaller than the one recorded in Figure 4B, a result consistent with the smaller R_0 value reported for the 510 nm QD−Cy3 pair compared to the 555 nm QD−Cy3 pair (see Figure 2). Last, Figure 4D shows deconvoluted spectra for the case where both QD−MBP conjugates are assembled with 4

MBP−Cy3 per QD; both QD emissions are quenched ($E_{555-Cy3} = 0.55$, $E_{510-Cy3} = 0.43$). The larger Cy3 PL signal collected from this sample reflects an energy transfer from both QD populations and is equivalent to about 90% of the sum of the individual Cy3 contributions shown in Figure 4B and 4C. In our present study, the number of labeled proteins around each QD was four ($n = 4$), and the measured values are close to those expected using eq 3 and the anticipated experimental values for r and R_0.

2. Three QD Donor Populations with QSY-7 Dark Quenching Acceptor. Figure 5A shows the composite spectrum collected from a sample of three QD populations (emitting at 510, 555, and 590 nm) conjugated to 15 unlabeled MBP, along with the deconvoluted individual PL contributions from each population. The QD concentration for each population was adjusted to provide comparable individual PL signals. This compensates for differences in absorption cross sections and fluorescence quantum yields among the QD populations used; more blue-emitting QDs tend to have smaller absorption cross sections than their red-emitting counterparts.[23,36−39] In this system, 510 nm QDs are more concentrated than 555 and 590 nm QDs. Although this PL normalization step is not strictly required for successful multiplexing, it allows a clear visual comparison of the relative PL changes for each QD population. Figure 5B shows the composite and deconvoluted spectra for the case where one QD−MBP population (510 nm QDs) is selectively dye-labeled. Data clearly show that emission from the 510 nm QDs is substantially quenched, but contributions from the other two QDs are nearly unaffected. Figure 5C shows selective quenching of the 510 and 555 nm emitting QD−MBP conjugates (due to selective labeling with QSY-7), with minimal effects on contribution from the unlabeled 590 nm QDs. These
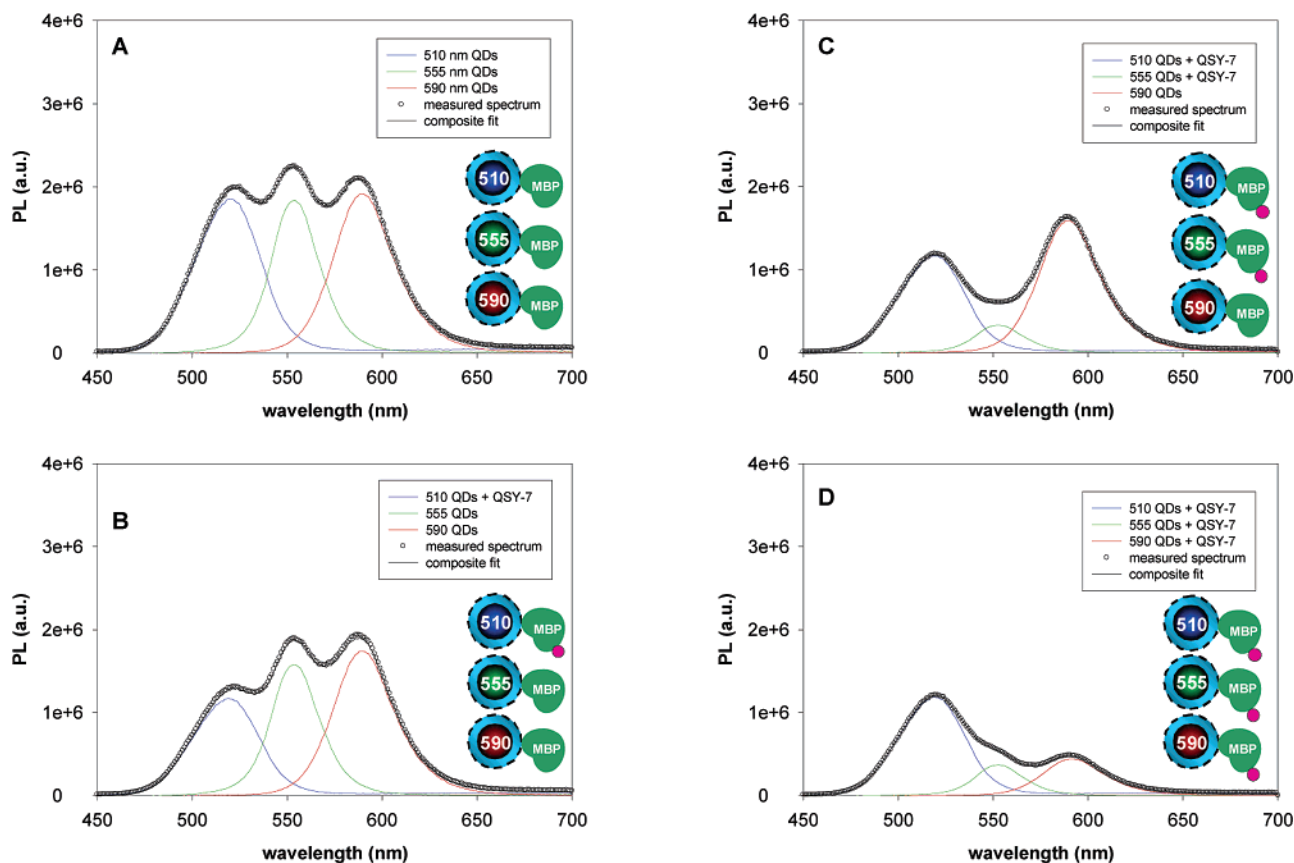
Figure 5. Deconvoluted PL spectra for the system using three QD donors interacting with QSY-7 quencher. The composite spectrum is shown as open circles (○), the fitted spectrum as a solid black line, and individual contributions as blue (510 nm QDs), green (555 nm QDs), and orange (590 nm QDs) lines. (A) Spectra for all unlabeled QD conjugates. (B) Only conjugates of the 510 nm QDs are QSY-7-labeled. (C) 510 and 555 nm QDs are conjugated to MBP−QSY-7. (D) All three QDs have dye-labeled MBP. Cartoons representing labeled and unlabeled QD conjugates are shown in the insets.

Table 1. Fitting Coefficients (Weighting Factors) for the Three QD Donor/QSY-7 Acceptor System[a]

configuration	510 nm QD	555 nm QD	590 nm QD
no quencher (A)	1.000	1.000	1.000
510 nm QD population quenched (B)	**0.635**[b]	0.857	0.918
510 and 555 nm QD populations quenched (C)	**0.639**	**0.178**	0.835
all populations are quenched (D)	**0.636**	**0.205**	**0.224**

[a] These coefficients provide a measure for the relative contribution of each QD population (color) to the composite spectrum compared to the initial dye-free solution in A. [b] Bold indicates a donor with bound MBP−QSY-7.

data further show the strong dependence of the quenching efficiency on the degree of spectral overlap between a particular set of QDs and QSY-7. In this case, both 510 and 555 nm emitting QDs have four labeled MBP per QD, but larger overlap between the 555 nm QD emission and QSY-7 absorption leads to a higher FRET efficiency for this pair. Figure 5D shows the composite and deconvoluted spectra from a sample where all three QD−MBP populations have four MBP−QSY-7; all three PL contributions are quenched. Fractional contributions of each QD population are summarized in Table 1 where cases A−D correspond to the results shown in Figure 5A−D, respectively. These values represent the fraction of QD PL remaining ($1-E$, see eq 1) for each of the four configurations. As expected, QDs conjugated to dye-labeled proteins (values shown in bold in Table 1) show pronounced fractional PL loss due to nonradiative

energy transfer. In comparison, smaller losses (due to diffusion-driven FRET) are measured for unlabeled QDs.

3. Four QD Donor Populations with QSY-7 Dark Quenching Acceptor. In this configuration we used the three populations above (510, 555, and 590 nm QDs) and added 570 nm QDs to the mixture. As in the previous arrangement, concentrations were adjusted to generate similar PL contributions from the various populations in the mixture. Figure 6A shows the composite spectrum together with the deconvoluted individual contributions from a solution mixture of QD−MBP conjugates, each with 15 unlabeled MBP per QD. Unlike the three QD multiplexed system above, it is not possible to visually distinguish individual contributions (i.e., emission peaks are obscured) in the composite spectrum, due to a pronounced overlap between the individual emission spectra. This highlights the need for an accurate method of signal deconvolution. Figure 6B shows quenching of the 570 nm QD−MBP population following selective labeling with four MBP−QSY-7. Deconvoluted contributions compared to spectra in Figure 6A reveal substantial quenching of the 570 nm QD signal, while signals from the other three QDs are nearly unaffected. Figure 6C, D, and E show composite and deconvoluted spectra collected from solutions where two, three, or all four QD−MBP populations were labeled with QSY-7 (at four MBP−QSY-7 per QD), respectively. The relative contributions of each QD PL signal to the total measured spectrum are summarized in Table 2 and expressed as fractions of the QD PL intensity measured for each population in a dye-free solution. As shown above in Table 1,
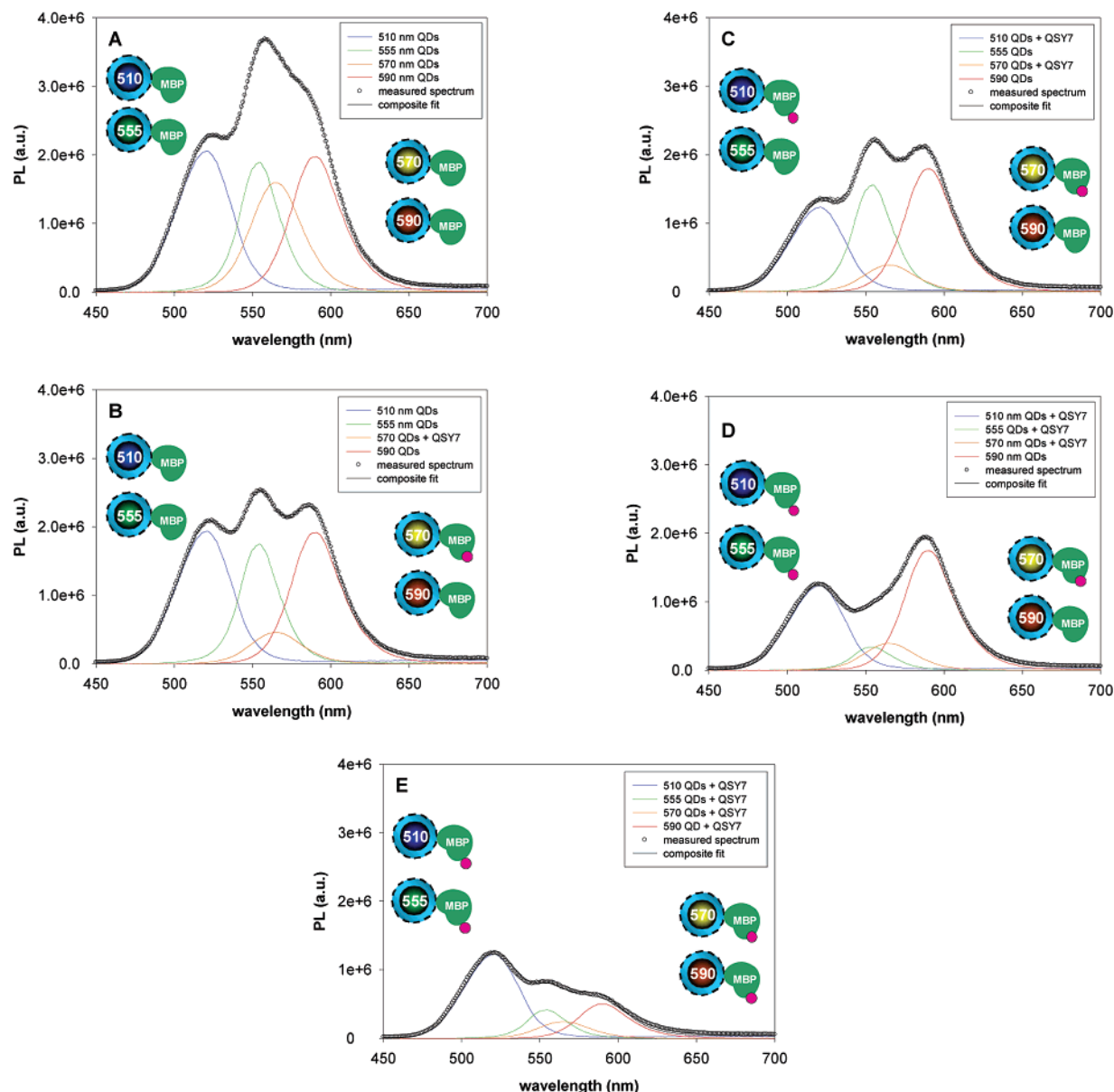
Figure 6. Deconvoluted spectra for the four QD donor−QSY-7 quencher system. (A) Spectra of 510, 555, 570, and 590 nm QDs, each with 15 unlabeled MBP per QD. The composite spectrum is shown as open circles (○), the fitted spectrum as a solid black line, and individual contributions to the fit as blue (510 nm QDs), green (555 nm QDs), orange (570 nm QDs), and red (590 nm QDs) lines. (B) Only conjugates of 570 nm QDs are QSY-7-labeled. (C) Conjugates of 510 and 570 nm QDs are QSY-7-labeled. (D) Conjugates of 510, 555, and 570 nm QDs are QSY-7-labeled. (E) Spectra where all four QD samples are QSY-7-labeled. Cartoons representing labeled and unlabeled QD conjugates are shown in the insets.

Table 2. Fitting Coefficients (Weighting Factors) for the Four QD Donor−QSY-7 Acceptor System[a]

configuration	510 nm QDs	555 nm QDs	570 nm QDs	590 nm QDs
no quencher	1.000	1.000	1.000	1.000
570 nm QD population quenched (B)	0.941	0.923	**0.286**	0.970
510 nm, 570 nm QD populations quenched (C)	**0.599**	0.823	**0.243**	0.909
510 nm, 555 nm, 570 nm QD populations quenched (D)	**0.601**	**0.180**	**0.245**	0.884
all populations quenched (E)	**0.597**	**0.219**	**0.152**	**0.253**

[a] These coefficients provide an experimental account for the relative contribution of each QD population (color) to the composite spectrum, compared to the initial dye-free solution containing all QD−MBP conjugates [b] Bold indicates a donor with bound MBP−QSY-7.

these values represent a measure of PL loss due to FRET for each individual population in the mixture. Quenching of the

PL in each case is selective, with only populations of QDs conjugated to dye-labeled MBP experiencing significant PL loss. Furthermore, the level of quenching of each QD emission is directly dependent on the degree of spectral overlap, with the maximum PL loss (or quenching) measured for the 570 nm QDs and the smallest recorded for the 510 nm QDs (consistent with calculated R_0 values, see Figure 2).

Fluorescence Lifetime Measurements. To confirm the steady-state observations of multiplexed FRET between several QD donors and a single dye acceptor, we carried out time-resolved fluorescence measurements of lifetime changes for individual donor QDs in a mixture. However, we limited our present experiments and analysis to the configuration having three QD donors and one QSY-7 acceptor. The present results are representative of what can be expected for the other configurations. Figure 7 shows the time-resolved spectroscopic
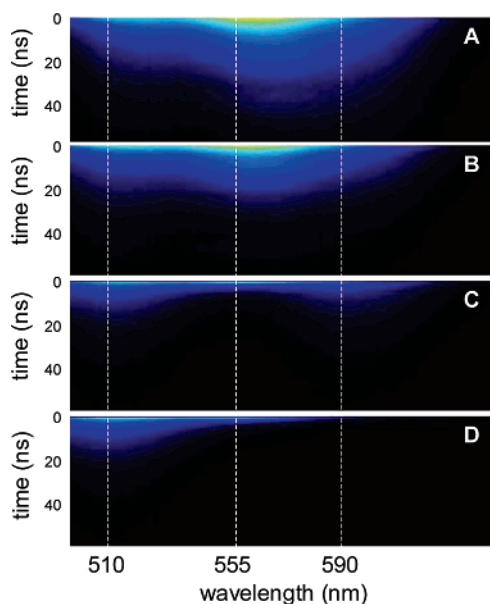
Figure 7. Composite time-resolved spectra recorded for the three QD donor−QSY-7 quencher system. (A−D) Lifetime spectra corresponding to the configurations depicted in Figure 3A−D, respectively. Wavelength is shown on the abscissa, and time, on the ordinate. Individual QD emission peaks are highlighted with white dashed lines at 510, 555, and 590 nm.

images of the fluorescence signals for the mixed sample collected at increasing time following a short excitation pulse; intensities are represented as contour colors (with intensity increasing from blue to red), wavelength is on the abscissa, and time increases down the ordinate. For clarity, dashed white lines are shown at the three emission maxima of 510, 555, and 590 nm. Figure 7A shows the time-resolved images for a sample composed of QD−MBP conjugates (each QD has 15 unlabeled MBP, no dye present). Figure 7B, C, and D, respectively, show time-resolved spectroscopic images for solutions where only 510 nm QDs were conjugated to QSY-7-labeled MBP, both 510 and 555 nm QD−MBP were dye-labeled, and a solution where all three QD−MBP populations were dye-labeled; a dye-to-QD ratio of 4:1 was used for each labeled population.

The data shown in Figure 7A−D were further processed to generate profiles for the fluorescence decay with time (see Figure 8A−C). Fits of the decay curves yield quantitative estimates of QD lifetimes for each configuration shown. Although full spectral deconvolution is difficult in this case (requiring processing of individual spectra at each time increment), we were able to specify and combine discrete regions of the composite spectrum that correspond to emission from individual QD populations. The binned wavelength regions provide intensity decays that are representative of individual QD signals. Figure 8A−C show intensity decays for each QD population in the multiplexed system, extracted from data shown in Figure 7A−D, as the labeling configuration was changed. Figure 8A, for example, shows the 510 nm QD fluorescence decay in the four configurations corresponding to Figure 7A−D. Data clearly show a pronounced lifetime decrease for each population when it is specifically conjugated to labeled MBP, independent of the labeling of other QD populations. Consistent with observations in steady-state fluorescence quenching, conjugation of 510 nm QDs to MBP−QSY-7 produces a smaller decrease in the decay lifetime as shown in Figure 8A due to relatively poor spectral overlap. Lifetime changes are more

pronounced for the other two populations upon conjugation to MBP−QSY-7 with each having better spectral overlap. In addition to the specific pronounced changes in the fluorescence decay when a population is directly labeled, additional (small) quenching effects are observed for a particular population in the presence of another labeled QD−MBP population (i.e., signal cross-talk). These effects are attributed to diffusion-driven energy transfer (see Discussion below).[42]

Discussion

The steady-state fluorescence results demonstrate that, in a biological context, where acceptors are brought in close proximity to the QD center via self-assembly with dye-labeled proteins, simultaneous energy transfer between QD donors and proximal dye acceptors can be realized and quantitatively analyzed. This multiplexed format is demonstrated with two configurations: one QD donor interacting with several distinct acceptors (Figure 1A) or multiple QD donor populations interacting with the same acceptor type (Figure 1B). Time-resolved fluorescence results corroborate the steady-state data with only the QD populations (in the mixture) engaged in nonradiative energy transfer and showing a significant decrease in radiative lifetime. This is in agreement with our previous findings where we have shown that steady-state and time-resolved experiments provide consistent information regarding nonradiative energy transfer between QDs and proximal dyes in a configuration using one donor and one acceptor pair.[18,23] The data presented in this study also show that our simple deconvolution algorithm permitted effective separation of individual steady-state PL contributions even when spectral separation between adjacent signal channels is small. This procedure is facilitated by the narrow and symmetric QD PL spectra.

There are several key differences between the two proposed multiplexing arrangements. The arrangement where multiple distinct MBP-dye acceptors are immobilized on the same QD donor (configuration 1, Figure 1A) provides steady-state data that require complex analysis. If changes in the QD PL are monitored alone, it is impossible to determine which proximal acceptor is contributing to the observed QD PL loss. It is therefore necessary in this arrangement to analyze signal changes of *both* the QD donor and dye acceptors. Using additional dyes requires more complicated spectral deconvolution because of the broad and often complex emission spectra of organic dyes. Moreover, nonradiative energy transfer between dyes attached to the same donor may be nonnegligible, further complicating the analysis. This motivated us to use a configuration where multiple QD populations are coupled to one acceptor type (configuration 2, Figure 1B) for FRET multiplexing. This alternate configuration has a few inherent advantages over configuration 1. The narrow and symmetric QD photoemission profiles allow a greater number of simultaneous signals to be spectrally separated into individual PL contributions. It is also much easier to detect FRET interactions between one particular QD population and the common acceptor by simply monitoring a change in QD PL (rather than having to analyze donor and acceptor PL changes); FRET channels are spectrally distinguishable from each other. Within this configuration we explored the case of two donors and one emitting acceptor and showed that the PL loss of each donor (each signal channel) can be quantitatively correlated to the degree of spectral overlap and reflected in the PL gain of the acceptor. In addition, when the
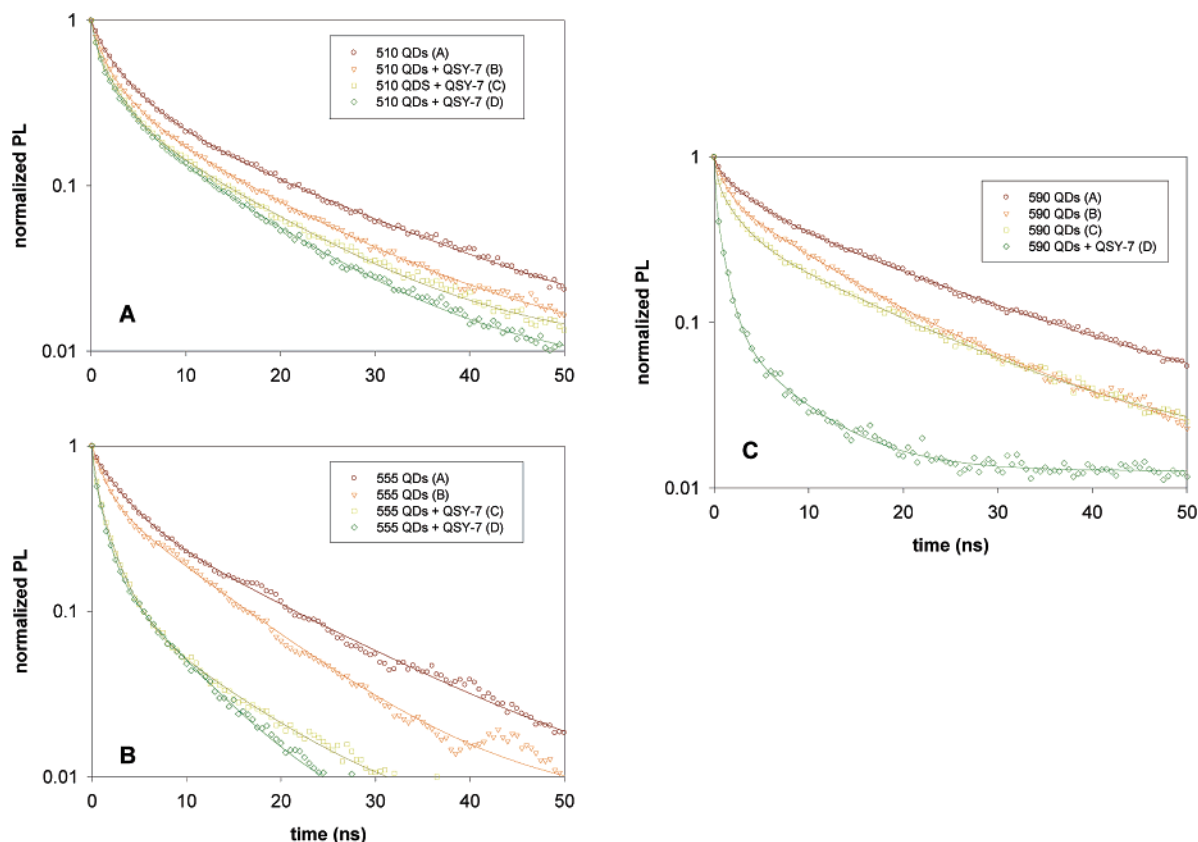
Figure 8. Plots of time-resolved fluorescence emission for the three QD donor−QSY-7 quencher system. (A) 510 nm, (B) 555 nm, and (C) 590 nm QD fluorescence decays isolated from the results shown in Figure 7A−D.

two donors are simultaneously engaged in FRET with the acceptor, the individual PL loss for each population is nearly identical to the loss measured when that channel is selectively interrogated (one isolated QD population is dye-labeled).

When three or more QD donors are used, a more judicious choice of a common acceptor is needed to maximize the degree of spectral overlap of all donors used with a finite acceptor absorption window. Furthermore, since a spectral deconvolution of a complex signal is involved, choosing a dark quenching rather than emitting dye acceptor can substantially simplify data processing. The asymmetric profile of emissive dyes presents an additional difficulty for spectral deconvolution. Our present set of data collected from the three and four QD multiplexed systems (in conjunction with one common QSY-7 acceptor) showed that we could readily account for three and four distinct FRET interactions, respectively.

In a multiplexed system involving more than one dye-labeled donor, additional FRET quenching of each population (including signal cross-talk) due to diffusion-driven proximity needs to be considered. However, these effects are typically small compared to quenching within self-assembled conjugates and usually increase linearly with quencher concentration, consistent with a Stern−Volmer model.[42] For the concentrations used in these systems (∼10 nM per QD population), the nonspecific quenching varied between ∼3% for the two channel multiplexing (two QD donors and one acceptor) and increased to ∼15% for the four channel multiplexing (four QD donors and one acceptor). Using lower overall concentrations while maintaining similar donor−acceptor ratios could further reduce these nonspecific quenching effects.

The results presented above demonstrating multiplexed FRET using luminescent QDs as energy donors to proximal dye acceptors have important implications for the future development of QD-based multiplexed sensors. They can be used as a basis for developing solution-phase sensing systems where multiple target analytes can be simultaneously detected. This complements our prior demonstrations of FRET-based QD sensing assemblies targeting either maltose sugar or soluble TNT.[18,25] Sensing formats based on FRET could be augmented to a multiplexed system to detect multiple target molecules in a sample using configuration 2 (shown in Figure 1B). The FRET multiplexing method discussed here differs from the sensing scheme using a sandwich fluoroimmunoassay format[19] in three fundamental ways. First, the sandwich assay uses direct fluorescence excitation only, where the detection of a target analyte occurs simply by measuring the PL intensity from the subset of QD−antibody conjugates bound to that analyte. Alternatively, the FRET-based technique uses changes in the PL signature of the QD−dye pair due to binding or releasing. Second, the FRET assay can use either freely diffusing or surface-immobilized QD bioconjugates to interact with an analyte in solution. The sandwich assay requires preparing surface-immobilized (capture) antibodies followed by exposure to analytes, QD conjugates, and subsequent rinsing steps prior to measurements. Third, FRET-based assays can monitor binding interactions as well changes in protein conformation, while fluoroimmunoassays are in principle limited to detect the former only.

We next discuss the advantages and potential hurdles of using our described approach to realize multiplexed sensing systems

based on QDs and FRET. The first consideration is the ability to resolve independent QD spectra using the deconvolution algorithm described. We have shown that emission spectra separated by only 15 nm in their intensity maxima (where the distributions have similar fwhm, here ~25−35 nm) can be resolved without difficulty. It is possible that this spectral separation can be reduced to 10 nm, but due to some inherent small spectral shift of the QDs, it will be difficult to further improve this resolution.[23] Additionally, using only CdSe−ZnS core−shell QDs imposes a limitation on the emission window from about 490 to 630 nm. Assuming we can resolve populations having emission maxima separated by 10 nm, this imposes an upper limit of about 15 independent signal channels. The second consideration is associated with the QD size. A FRET-based signal transduction mechanism requires small donor−acceptor distances for efficient energy transfer (smaller than ~$2R_0$). QDs having emission maxima above approximately 600 nm have relatively large core sizes, which produces modest to weak FRET efficiencies. Expanding the accessible spectral window would require either a different binary core material or perhaps doping the QD core to engineer significant spectral shift while maintaining a constant size that is conducive to FRET.[20,21] Even with a limited peak emission range of around 100−150 nm, such a system requires at least two types of dye acceptors to successfully quench the entire range of QD populations. In our system of four QD donors, QSY-7 alone has an absorption band broad enough to provide substantial spectral overlap with QDs having peak emissions spanning ~80 nm. Other dark quenchers (e.g., the BHQ or QXL dye series) may be considered when the dye acceptor is chosen to best match its QD donor counterpart. This methodology is not particularly sensitive to the specific dye used since only the QD PL is considered. The third and perhaps most important consideration is the choice of a recognition biomolecule to immobilize on the QD. A multiplexed sensing system requires biomolecules (e.g., proteins, peptides, antibodies, nucleic acids) that are highly sensitive and specific for target molecules of interest; these biomolecules must tightly bind to QDs and form stable bioconjugates. Using the flexible metal-affinity self-assembly process, we have successfully attached a variety of proteins and antibodies specific for sugars, toxins, and explosives. This strategy also requires that the bound proteins retain their native properties while attached to the QD surface. However, not all biomolecules are assured to behave in this way, which may limit the actual number of independent sensors available for multiplexing. Additionally, the sensing strategy based on displacement and PL recovery requires that a suitable analogue−dye conjugate can be prepared (e.g., TNB−BHQ10 for TNT used in ref 25) that will bind the biomolecule and be readily and specifically displaced.

Ultimately, FRET-based multiplexing with QD donors is not limited to a specific sensing scheme and may be generally applicable to a variety of strategies including competition/displacement, enzymatic digestion, aptamer-based molecular beacons, and reagentless sensing methods. Enzymatic activity could be analyzed by monitoring changes in the FRET signature as the target enzyme interacts with a QD conjugated to a dye-labeled substrate (e.g., proteins or peptides). As the substrate is consumed/cleaved, FRET efficiency is reduced resulting in QD PL recovery. In an aptamer or molecular beacon format, the presence of a target sequence or molecule would reconfigure the initial beacon structure due to specific interactions between the bioconjugate and target molecule. This rearrangement significantly alters the distance between the donor and acceptor and changes the measurable FRET signal. In both cases, the signal changes can be monitored as a function of the target concentration. Alternatively, the QD itself could be attached to a dye-labeled antigen or a target molecule.

Conclusions

We have demonstrated the ability to simultaneously monitor independent FRET interactions between specific QD donor populations conjugated to dye-labeled protein acceptors in a multiplexed arrangement. We explored two particular configurations: (1) a single QD is conjugated to multiple distinct dye acceptors and (2) multiple distinct QD donors interacting with the same dye acceptor. Our results indicate that although both cases allow simultaneous FRET interactions to be detected, configuration 2 combined with a quenching dye acceptor allowed for accurate spectral deconvolution by removing the dye contribution and simplified FRET analysis by requiring only a measurement of loss or recovery of QD emissions. Our study showed that when QD populations are conjugated to dye-labeled proteins, a pronounced and specific decrease in PL intensity of that population is measured, whereas the emission from unlabeled QDs was minimally affected. In particular, using a common acceptor (a QSY-7 dark quencher), we showed that up to four FRET interactions could be simultaneously measured using four QD populations conjugated to QSY-7-labeled MBP. These results suggest that a multiplexed sensing assembly based on FRET could be implemented to detect several target molecules in a given sample, extending our previous demonstrations using a single FRET channel to detect a single target analyte.

Supporting Information Available: Figure showing the composite spectrum for the single QD donor (555 nm QD)−two dye acceptor (Cy3 and QSY-7) system corresponding to the data shown in Figure 3. Unprocessed (not deconvoluted) spectra are shown to demonstrate the complexity of composite signals generated using configuration 1 in conjunction with an emissive dye acceptor. Proper analysis for such a system requires collecting accurate data for both the donor and emissive acceptors. These materials are available free of charge via the Internet at http://pubs.acs.org.

JA054630I